HOW MOLECULAR STRUCTURE AFFECTS MECHANICAL PROPERTIES OF AN ADVANCED POLYMER*

Lee M. Nicholson†, Karen S. Whitley, Thomas S. Gates and Jeffrey A. Hinkley

†National Research Council Resident Research Associate
NASA Langley Research Center, Hampton, VA 23681-2199

ABSTRACT

Mechanical testing of an advanced polymer resin with known variations in molecular weight and cross-link density was performed over a range of temperatures below the glass transition temperature. The physical characterization, elastic properties and notched tensile strength all as a function of molecular weight and test temperature were determined. For the uncrosslinked SI material, it was shown that notched tensile strength is a strong function of both temperature and molecular weight, whereas stiffness is only a strong function of temperature. For the crosslinked PETI-SI material, it was shown that the effect of crosslinking significantly enhances the mechanical performance of the *low* molecular weight material; comparable to that exhibited by the *high* molecular weight material.

KEY WORDS: Polymeric Resin Matrices, Mechanical properties, Modeling.

1. INTRODUCTION

Modern tendencies in the design and production of advanced structural materials strive for optimal mechanical properties with a minimum of weight. State-of-the-art polyimides in conjunction with reinforcing components such as graphite fibers create novel polymer matrix composites (PMC's). In airframe structure, these PMC's can give up to 40% weight savings, along with a reduction in the number of parts [1].

Failure or degradation of performance in PMC's is usually associated with loss in mechanical load carrying capability of the polymer matrix. Early experiments by Nielsen [2] on atactic polystyrene have shown that below the glass transition temperature (T_g) the relative effect of molecular weight on mechanical properties increases as the experimental regimen moves from elastic to viscoelastic to large strain and finally fracture testing. Matsuoka [3] noted that in the glassy state, the molecular weight affects the toughness and impact strength of the polymer; impact strength increases with molecular weight. Walsh and Termonia studied the dependence of fracture toughness on molecular weight and test temperature for poly(methyl methacrylate)[4]. They found that changes in fracture toughness were strongly dependent on the temperature and on the molecular weight distribution.

Despite the relevance of this afore-cited literature, there is still no unified understanding of exactly how the intrinsic chemical and physical properties of the polymer affect the resultant mechanical performance. The ability to predict performance using intrinsic properties as inputs would greatly enhance the efficiency of design and development of PMC's. Data from experiments can serve as a basis for model construction and provide material properties required by the selected model. One of the first steps in the construction of a model is the careful experimental correlation of thermo-mechanical behavior of a well-characterized polymer to known changes in intrinsic properties.

Aromatic polyimides are thermally stable high performance polymers that are used in a variety of commercially available forms: composite matrices, adhesives, coatings, films and fibers [5]. However, the polyimide is often difficult to process by compression molding owing to its infusible nature. To overcome this shortcoming, imide oligomers terminated with reactive phenylethynyl groups have been shown to cure at high temperatures (~370°C) without the evolution of volatiles, thus offering a larger processing window [6-12]. Upon thermal cure, the phenylethynyl group undergoes a complex reaction that involves chain extension and crosslinking proceeding via free-radical mechanisms. It would be desirable to understand what impact the crosslink density has on the mechanical performance on this polymer system.

The objective of this paper is to detail and summarize the physical and mechanical testing of an advanced polymer (LaRC™-SI) and its cross-linked form (LaRC™-PETI-SI). Using five known variations in molecular weight and cross-link density, static tests were performed over a range of temperatures below the glass transition. Results from these tests will be presented along with descriptions of the material and test methods.

2. EXPERIMENTAL

2.1 Materials The materials used in this study were prepared by Imitec Inc., Schenectady, NY, and received in powder form. LaRC™-SI (NASA Langley Research Center-Soluble Imide) was synthesized from 4,4'-oxydiphthalic anhydride (ODPA), 3,3',4,4'-biphenyltetracarboxylic dianhydride (BPDA) and 3,4'-oxydianiline (3,4'-ODA). Stoichiometric imbalances, designated by their percent offsets [13], were prepared by reacting an excess of the diamine with an appropriate quantity of the dianhydrides in *N*-methyl-2-pyrrolidinone (NMP). Extended synthesis descriptions of this material have been published elsewhere [14, 15]. The cross-linked form of the material is LaRC™-PETI-SI, where the PhenyEthynyl Terminated Imide was formulated with imide oligomers end-capped with 4-phenylethynylphthalic anhydride (PEPA) [11]. Molecular weights were determined on the as-received powders using gel permeation chromatography [13]. The weight-average molecular weight ($\overline{M_w}$) and the polydispersity index of the SI and PETI-SI samples are shown in Table 1 and Table 2, respectively. The differences in the molecular weight distribution per sample, are more easily discerned when weight averages are compared.

2.1.1 Characterization The powder was dried under vacuum at 215°C for 48 hours to remove any residual solvents prior to being compression molded in air. The powder was placed in a 152 x 152 mm stainless steel mold lined with Kapton™ film spray-coated with Frekote 33-NC release agent. Neat resin plaques were formed at 340°C for one hour under 3.1 MPa of pressure. Mechanical test coupons measuring approximately 150 x 17.5 x 5.8 mm were machined from the plaques. Differential scanning calorimetry (DSC) was performed using a Perkin Elmer DSC 7 to determine the glass transition temperature (Tg) of the cured material. Polymer sample weights of 2-5 mg were used under a nitrogenous atmosphere at a heating rate of 10°C/min. The glass transition temperature was taken at the inflection point in the heat flow versus temperature curve.

Rheological measurements were conducted on a Rheometrics System 4 rheometer. Sample specimen disks, 2.54 cm in diameter and ~1.5 mm thick, were prepared by press molding the powder at room temperature. The compacted resin disk was then loaded in the rheometer fixture with 2.54 cm diameter parallel plates. The top plate oscillated at a fixed strain of 5%, and a fixed angular frequency of 10 radians/s, while the lower plate was attached to a transducer that recorded the resultant torque. The temperature was recorded in a range from room temperature to 400°C at a heating rate of 4°C/min. Dynamic storage (G') and loss (G'') moduli were measured as a function of time (t) at several key temperatures.

2.2 Static Test Instrumentation and Procedures The goal of the static tests was to determine the elastic properties, and notched tensile strength as a function of molecular weight, test temperature and cross-link density. Static tensile tests were performed at six specific test temperatures below the glass transition temperature (T_g). The T_g's for each molecular weight are shown in Table 1. To place equal emphasis on the results, the temperature is referenced to the difference between glass transition and test temperature, as defined below:

$$\Delta T = T_g - T_{test} \tag{1}$$

% Offset	$\overline{M_w}$ (g/mol)	$\frac{\overline{M_w}}{\overline{M_n}}$	T_g (°C) (cured)	ΔT = 15 K	ΔT = 25 K	ΔT = 45 K	ΔT = 70 K	ΔT = 120 K
1	51070	4.57	250	235	225	205	180	130
2	41100	2.98	246	231	221	201	176	126
3	24290	2.30	238	223	213	193	168	118
4	21180	2.04	238	223	213	193	177*	126*
5	15880	1.79	234	219	209	189	164	114

Table 1. Static Test Temperatures (°C) and molecular weights for SI specimens. ($\Delta T = T_g$ – Test Temperature); * The actual test temperatures deviated from ΔT.

% Offset	$\overline{M_w}$ (g/mol)	$\frac{\overline{M_w}}{\overline{M_n}}$	T_g (°C) (cured)	ΔT = 15 K	ΔT = 25 K	ΔT = 45 K	ΔT = 70 K	ΔT = 120 K
4	31275	3.03	258.7	243.7	233.7	213.7	188.7	233.7
5	24290	2.75	261.5	246.5	236.5	216.5	191.5	141.5
7	15410	2.45	256	241	231	211	186	136
9	10850	2.27	264	249	239	219	194*	144*
11	8743	2.04	262	247	237	217	192	142

Table 2. Static Test Temperatures (°C) and molecular weights for PETI-SI specimens. ($\Delta T = T_g$ – Test Temperature); * The actual test temperatures deviated from ΔT.

Uniaxial tensile tests were performed using a 22.2 kN servo-hydraulic test system equipped with a heated test chamber. The specimens were enclosed in the chamber and mounted in mechanical wedge type grips. During the course of a test, temperature was monitored with several thermocouples placed near the specimen. The test temperature was stabilized first and then a tensile load was applied at a constant ramp rate of 22.2 N/s. The tests were terminated when failure occurred or the desired elongation was achieved.

A high-temperature strain gage was applied to each specimen in a direction transverse to the length on the face of the specimen. The specimen and gage were subsequently dried at 110°C for 120 hours and post-cured at 210°C for 2 hours. Longitudinal strain was measured using an extensometer mounted on the thin edge of the specimen. The output voltages from the strain gages were filtered and amplified by a strain gage conditioner before the conditioned output was collected by the digital data acquisition system.

The engineering stress on the specimen was determined from the load measured by the servo-hydraulic system's load cell divided by the average cross-sectional area measured prior to the test. Each recorded elastic modulus measurement is an average of at least three replicates of each molecular weight at each test temperature.

2.2.1 Notched Tensile Strength For a given molecular weight, only two tests at each temperature were made using the notched specimen geometry. To facilitate a controlled failure, an edge notch was cut in the specimen using a jeweler's blade (0.38 mm width) mounted on a handsaw. The notch was placed on one side only, at 44 mm from the bottom grip and extended approximately 2 mm in from the free edge. Tensile strength was calculated from the maximum load achieved during the tensile test divided by the original, unnotched cross sectional area. Photomicrographs were taken of the notched surface after failure to determine the morphology of the failure surface (shown in fig. 6).

2.2.2 Elastic Properties Young's Modulus, (E) was calculated using equation (2) from the least squares fit to the slope of the linear portion of the stress, (σ), versus the longitudinal strain, (ε_x), curve. Similarly, Poisson's Ratio (ν), equation (3), was calculated as the slope of the transverse strain (ε_y), versus the longitudinal strain in the same linear region. Shear Modulus (G), equation (4), was calculated in terms of E and ν.

$$E = \frac{\sigma}{\varepsilon_x} \tag{2}$$

$$\nu = -\frac{\varepsilon_y}{\varepsilon_x} \tag{3}$$

$$G = \frac{E}{2(1+\nu)} \tag{4}$$

3. RESULTS AND DISCUSSION

3.1 Molecular Weight The experimental results are presented for all the measured static behavior on the SI specimens. All results have been examined by comparing the property of interest to variations in test temperature and molecular weight. The error bars indicate the standard deviation of averaged results.

3.1.1 Elastic Properties Young's Modulus (E) and Shear Modulus (G) versus temperature are given in figure 1. As expected, both E and G decrease as temperature is raised. The rate of change of E with temperature is fairly uniform up to 200°C. From 200°C to the highest temperature (~235°C) there was a sharp decrease in modulus because the temperature was in the vicinity of the softening point of the material. In accord with Young's Modulus, G decreases in a uniform manner as the temperature is raised, but with a shallower gradient. The start of the sharp decrease in modulus occurs at a higher temperature of ~220°C. Common to both data sets is the fact that the low molecular weight materials lose their mechanical properties at a slower rate initially than the high molecular weight material.

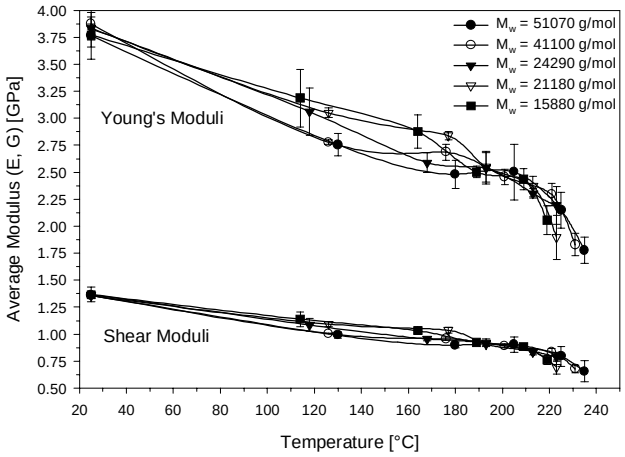

Figure 1. Averaged Young's and Shear moduli plotted as a function of temperature for various molecular weights.

The variations of E and G with molecular weight are shown in figures 2 and 3, respectively. It can be seen that there is not a strong dependence of the Young's Modulus or Shear Modulus on molecular weight. However, there is a small change occurring between 22000 and 25000 g/mol molecular weight in both the Shear and Young's Moduli of the ΔT =70 K curve. In addition, both figures illustrate the temperature dependence on each modulus.

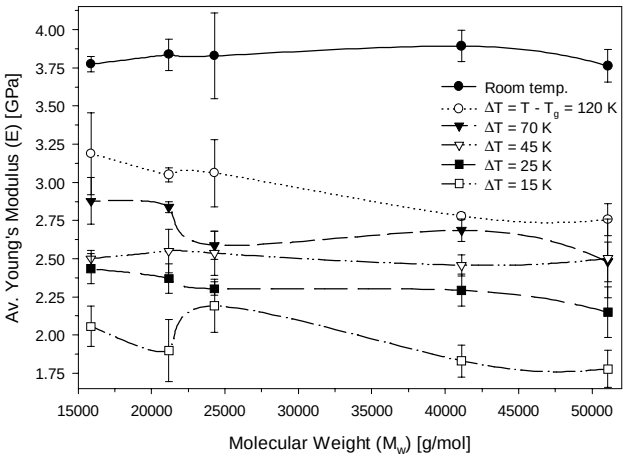

Figure 2. Averaged Young's moduli plotted as a function of molecular weight at various temperature intervals.

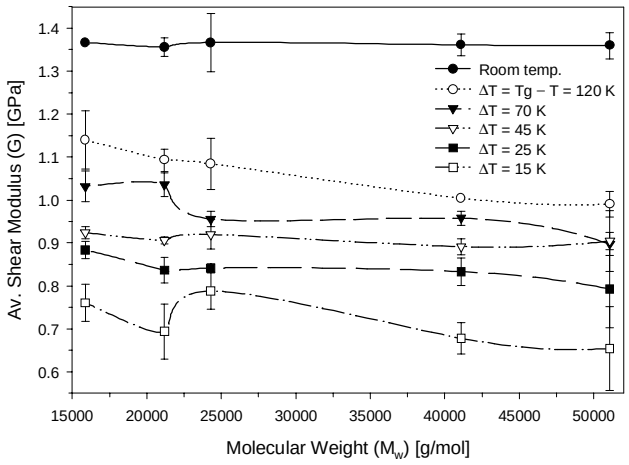

Figure 3. Averaged Shear moduli plotted as a function of molecular weight at various temperature intervals.

Notched tensile strength (NTS) versus temperature and molecular weight are shown in figures 4 and 5, respectively. Figure 4 illustrates the strong dependence of NTS on temperature. In general, NTS decreases as temperature increases. Over the range from room temperature to 150°C, the two highest molecular weight materials show a much lower rate of change in NTS compared to the lower molecular weight materials. However, in the range from 150°C to 230°C the converse is true with the lower molecular weight materials showing a lower dependency of NTS on temperature than the high molecular weight materials. Furthermore, the NTS of the high molecular weight materials declines rapidly in this high temperature region.

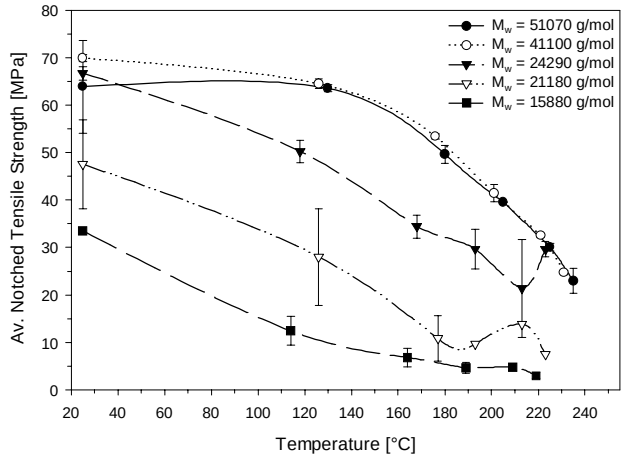

Figure 4. Averaged Notched Tensile Strength plotted as a function of temperature for various molecular weights.

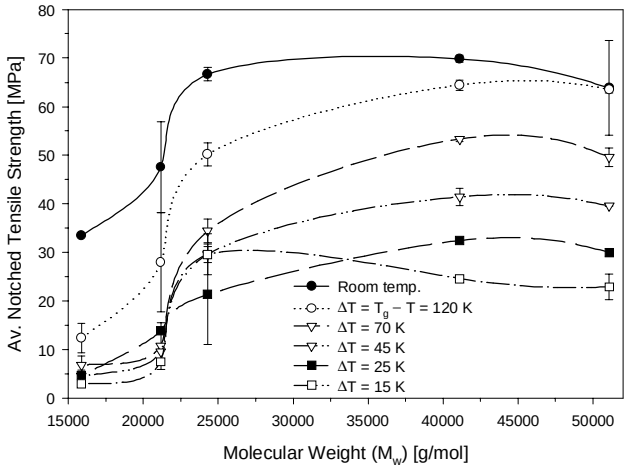

Figure 5. Averaged Notched Tensile Strength plotted as a function of molecular weight at various temperature intervals.

The data on NTS versus molecular weight, as shown in figure 5, indicate a sharp change in NTS occurring about 22000 g/mol molecular weight. At this transition the higher temperature data series exhibit a larger change in the NTS, as much as 300%, compared with 150% change at room temperature. At molecular weights higher than this "critical molecular weight", the NTS is increased and conversely, at lower molecular weights the NTS is reduced. There is a marginal drop in NTS at the highest molecular weight.

3.1.2 Fractography Additional evidence on the effects of temperature and molecular weight was obtained by examination of the failure surface. The photomicrographs of the notched surface after failure are provided in figure 6 for selected materials and temperatures. A failure surface was classified as ductile if the photomicrograph showed evidence of material elongation and smooth, glassy looking surfaces. The evidence of sharp edges and multiple crack sites can define a brittle failure. Figure 6 displays nine microstructural images characterizing the failure surfaces at various labeled points on the NTS versus molecular weight curve for three selected temperature intervals. Regarding the low molecular weight material (images: a, d, g) and the high molecular weight material (images: c, f, i), it can be seen that there is a marked transition from a brittle failure mode to a ductile failure mode. Upon examination of the images tracing a temperature series of NTS, it can be seen that there are distinct differences in the failure surfaces for different molecular weight materials. This is more clearly expressed in the interpolated surface plot of figure 7. Here, the dominant mechanical property of NTS is conveniently summarized in one diagram expressed as functions of molecular weight and temperature.

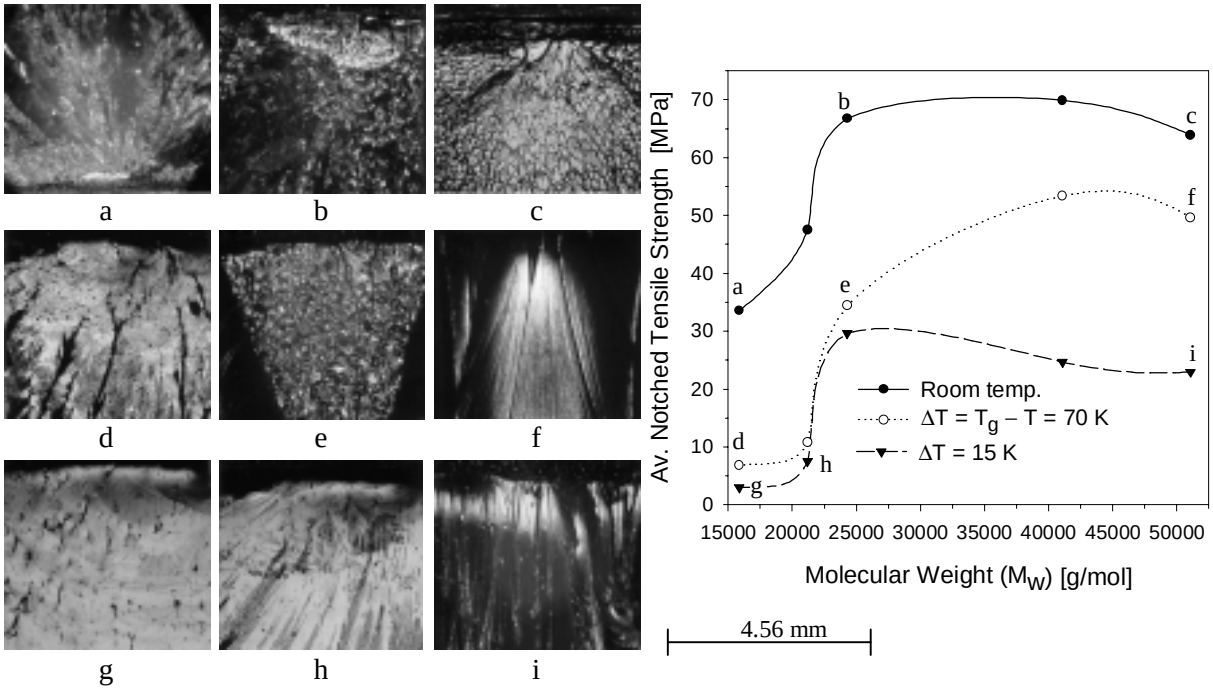

Figure 6. Microstructural images taken of the fracture surface corresponding to the appropriately indicated regions on the NTS versus molecular weight curves for selected temperature intervals.

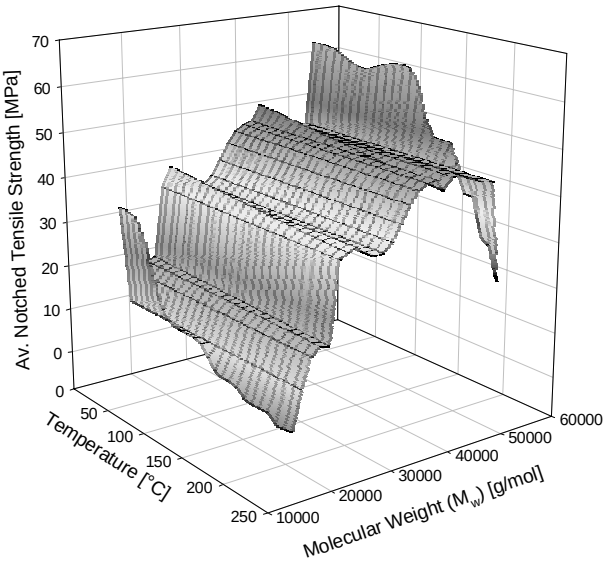

Figure 7. An interpolated 3D surface mesh interrelating temperature and molecular weight with NTS.

3.2 Cross-linking Density The experimental results are presented for all the measured static behavior on the PETI-SI specimens. All results have been examined by comparing the property of interest to

variations in test temperature and molecular weight. In a later section, the extents of the network properties are discussed. The error bars indicate the standard deviation of averaged results.

3.2.1 Elastic Properties Young's Modulus (E) and Shear Modulus (G) versus temperature are given in figure 8. As expected, both E and G decrease as temperature is raised. The rate of change of E with temperature is fairly uniform up to 240°C. From 240°C to the highest temperature (~250°C) there was a sharp decrease in modulus because the temperature was in the vicinity of the softening point of the material. In accord with Young's Modulus, G decreases in a uniform manner as the temperature is raised, but with a shallower gradient. The start of the sharp decrease in modulus occurs at the same temperature (240°C). Unlike the SI material, there is no clear distinction on the rate of loss of mechanical properties as a function of molecular weight.

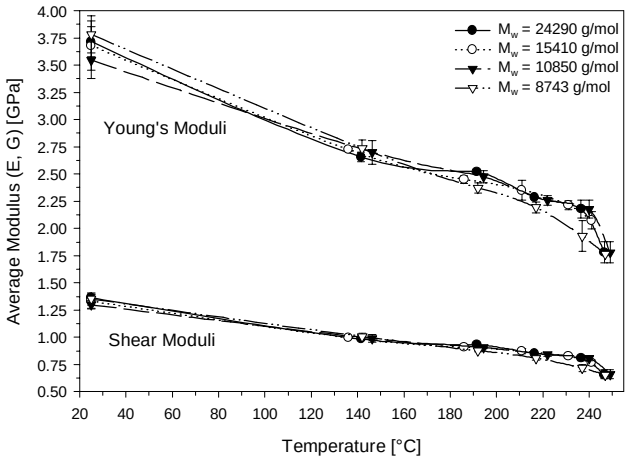

Figure 8. Averaged Young's and Shear moduli plotted as a function of temperature for various molecular weights.

The variations of the Shear and Young's Moduli with molecular weight are shown in figures 9 and 10, respectively. It can be seen, in accord with the SI material, that there is not a strong dependence of the Young's Modulus or Shear Modulus on molecular weight. However, there is a slight change in the modulus at 15410 g/mol in both E and G for the ΔT =15 K curve. In addition, both figures illustrate the strong temperature dependence on each modulus. In comparison with the SI material (figs. 2 & 3) in the low molecular weight range, it appears that the crosslinking has "smoothed out" the drop in both E and G occurring between 22000 and 25000 g/mol.

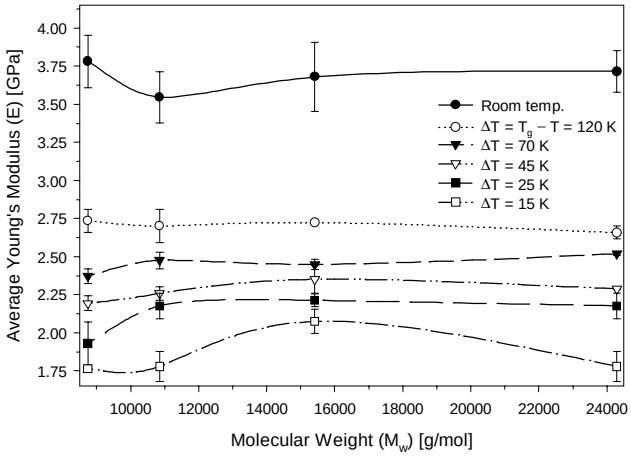

Figure 9. Averaged Young's moduli plotted as a function of molecular weight at various temperature intervals.

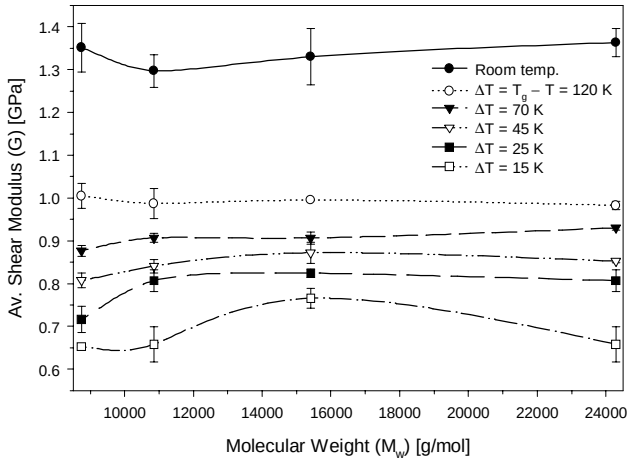

Figure 10. Averaged Shear moduli plotted as a function of molecular weight at various temperature intervals.

Notched Tensile Strength versus temperature and molecular weight are shown in figures 11 and 12, respectively. Figure 11 illustrates the dependence of NTS on temperature. In general, NTS decreases as temperature increases for all molecular weights of the PETI-SI material. Unlike the SI material, there is no molecular weight dependency in NTS or temperature dependency for a specific molecular weight (change in the curve shape). Over the temperature range from room temperature to 160°C, the PETI-SI materials show a much lower rate of change in NTS than in the range from 160°C to 250°C, where it declines more rapidly. This latter trend is consistent with only the high molecular weight SI materials (M_w > 24290 g/mol).

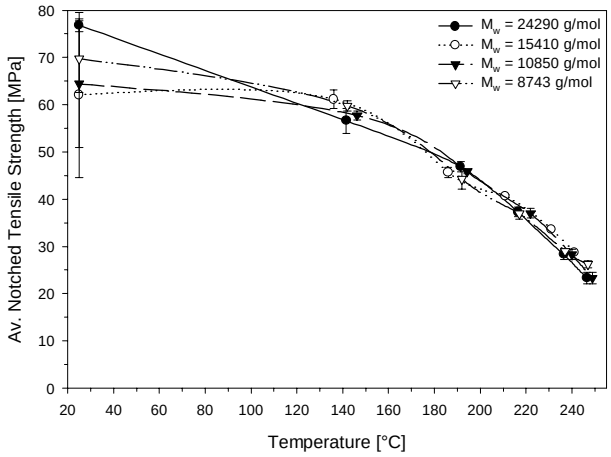

Figure 11. Averaged Notched Tensile Strength plotted as a function of temperature for various molecular weights.

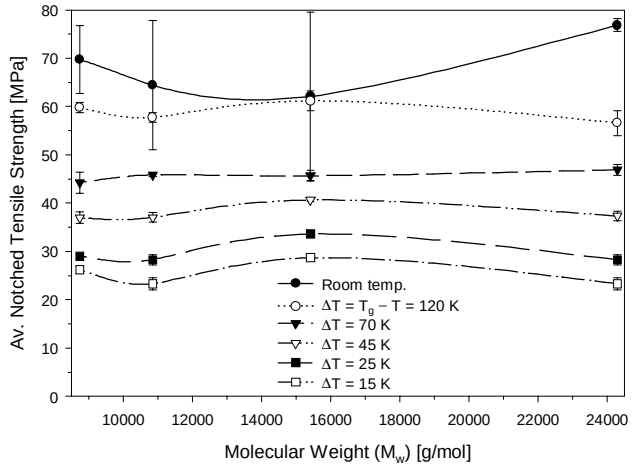

Figure 12. Averaged Notched Tensile Strength plotted as a function of molecular weight at various temperature intervals.

The data on NTS versus molecular weight, as shown in figure 12, indicate no change in NTS at a "critical molecular weight" as was observed with the SI materials. Unlike the SI materials, the NTS values for the PETI-SI materials are a factor of 2-5 times higher for the equivalent molecular weight range. However, there is some minor degree of sensitivity in NTS at a very low molecular weight. The large error bars on the room temp. curve indicate that there may be the involvement of different molecular-weight-dependent brittle fracture mechanisms, at the microstructural level, despite the small sample size in the error calculation.

3.2.2 Cross-linking effects on T_g The cure of phenylethynyl-terminated oligomers may be followed by the disappearance of phenylethynyl functionality [16, 17], but little is known about the exact crosslinking chemistry. Early in the reaction of monofunctional model compounds, dimer, trimer,

tetramer and insoluble products are formed [17]. On this basis, it would be expected that chain extension and crosslinking in PETI-SI would lead to the formation of an infinite network. Because the resin is insoluble, however, there are few experimental techniques available to quantify the degree of crosslinking. In the following, we describe two techniques: the first involves following the glass transition temperature.

3.2.2.1 Theoretical estimation of crosslink density Changes in T_g arise both from disappearance of chain ends and from the formation of chemical crosslinks [18]. Figure 13 illustrates the effect of chain ends on T_g in the PETI-SI series. The extrapolation shows that a PETI-SI material of infinite molecular weight (such as would result from chain extension only) would have a T_g of 258.82°C.

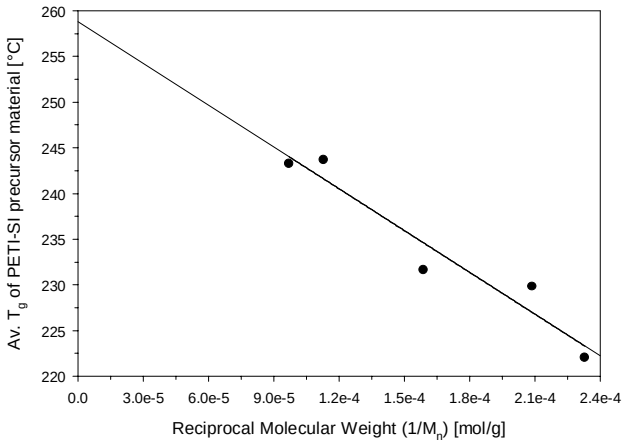

Figure 13. Averaged T_g of uncrosslinked PETI-SI material (prior to cure) versus reciprocal number average molecular weight.

Assuming all the phenylethynyl groups react, the difference between this and the observed T_g's of the cured resins is attributable to the additional reduction in entropy caused by crosslinks; for which, a relationship was derived by DiMarzio (DM)[19].

$$\frac{T(X)-T(0)}{T(0)} = \frac{KMX/\gamma}{1-KMX/\gamma} \qquad (5)$$

where *T(X)* is the Tg of the crosslinked material, *T(0)* the Tg of the uncrosslinked material, $K = 1.3 \times 10^{23}$, *M*, the molecular weight of the imide repeat unit (466.4538 g/mol), *X*, the degree of crosslinking , γ is the number of flexible bonds per repeat unit (4.5). Applying the DM equation to our data, the results in Table 3 suggest a very low degree of crosslinking, a result consistent with the mechanical properties in figures 8 and 11.

% Offset	$\overline{M_n}$ (g/mol)	$\overline{M_w}$ (g/mol)	DiMarzio -X (g^{-1})	DiMarzio-M_c (g/mol)	Rheology-G´ (Pa)	Rheology -X (mol/g)	Rheology-M_c (g/mol)
5	8841	24290	6.925×10^{18}	86965	2.07×10^{5}	2.76×10^{-4}	3619
7	6289	15410	6.390×10^{18}	94240	1.40×10^{5}	1.87×10^{-4}	5357
9	4786	10850	1.678×10^{19}	35895	5.74×10^{5}	7.65×10^{-5}	13066
11	4292	8743	1.103×10^{19}	54619	9.07×10^{5}	1.21×10^{-4}	8269

Table 3. Calculated and experimental values of the crosslink density (X) and molecular weights between crosslinks (M_c) for the various PETI-SI materials.

3.2.2.2 Rubber Elasticity A second approach to characterizing our networks applies rubber elasticity theory [20, 21]. Above T_g, the equilibrium shear modulus of a network is given by,

$$G_e = \nu_e RT \qquad (6)$$

where ν_e is the concentration of "elastically effective" chains, R is the universal gas constant, and T is the absolute temperature. Even in a simple, regular tetrafunctional network, there is some disagreement about the relationship between ν_e and crosslink density arising from the role of "junction fluctuations." In addition, our polyimide chains are highly entangled, so the equilibrium modulus may contain a contribution from trapped entanglements. Despite these uncertainties, it is interesting to compare the measured moduli of the cured PETI-SI materials using the dynamic shear modulus from Rheology data taken at 400°C. Apparent molecular weights between crosslinks, M_c, were calculated as ρ/ν_e, where the average polymer density (ρ) was taken as 1.34 g cm^{-3}. Comparing the M_c values, in the final column of Table 3, with the number average molecular weight of the polymer in column one, it can be seen that the two lowest molecular weight materials appear to be lightly crosslinked. However, the two largest molecular weights show moderate crosslinking density, a consequence possibly due to increased entanglement effects in the dynamic measurement of G_e.

3.2.2.3 Defining network properties Miller and Macosko [22] proposed a useful formalism for calculating network properties in gelled polymers. Ignoring entanglement effects for a moment, it is a straight forward exercise to calculate the probability that a reacted chain end is a part of an effective crosslink. This probability, in turn, depends on the extent of reaction and the average number of phenylethynyl groups that make up a crosslinking "node". Based on IR measurements [17], it is reasonable to assume complete consumption of phenylethynyl groups, or 100% reaction. The degree of polymerization ($\overline{dp_n}$) at the crosslinks is unknown, but in an ethynyl model compound, it was shown to be 5±0.5 [23]. At this degree of polymerization, many chain ends are linked to only one other, and thus participate in chain extension – not crosslinking. Calculation shows that at a ($\overline{dp_n}$) of 5, about half the initial chains are likely to be elastically active (figure 14). This is consistent with the low experimentally derived M_c values as compared with the theoretically calculated values in Table 3. A more detailed study of rubbery moduli is currently underway.

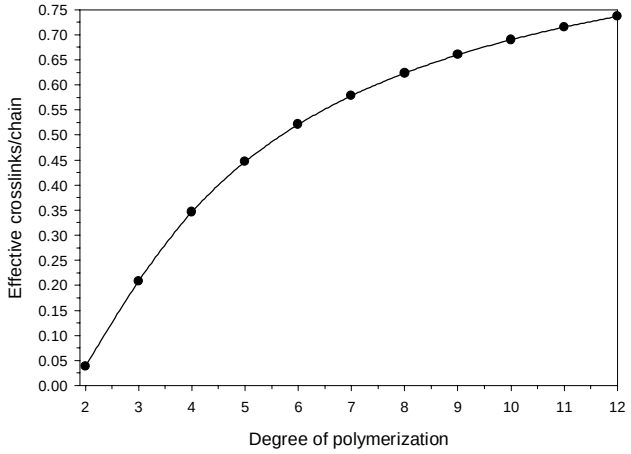

Figure 14. Number of effective crosslinks per chain as a function of degree of polymerization.

3.2.3 Summarizing network characterization The estimation of the crosslink density using DiMarzio's theory with the experimentally determined values of T_g for cured resins, suggests that the PETI-SI material is lightly crosslinked and mainly chain-extended. These large values given for M_c in Table 3 serve as an upper bound in estimating the degree of crosslinking. Using experimentally determined dynamic shear moduli in the classical rubber elasticity theory, suggests that the molecular weight between entanglements is much less than that calculated by DiMarzio's theory. By comparison with the number average molecular weight, determined experimentally by gel permeation chromatography, it can be seen that the values for M_c determined by rheology, are still an average of a factor of two less. This factor of two can be accounted for by using Miller and Macosko's theory on the "effectiveness" of a crosslinking reaction, which for an ethynyl model compound, suggests that only half the reactive crosslinking groups will produce effective crosslinks.

4. CONCLUSIONS

The physical characterization and the mechanical response of an advanced polymer have been determined. The observed microstructures have helped to characterize further the brittle to ductile transition as a function of molecular weight. Evidence from the experimental validation on SI material suggests that the notched tensile strength is a strong function of both temperature and molecular weight. The Young's modulus and Shear modulus are strong functions of temperature, but weak functions of molecular weight.

For optimal material selection and part design, the results suggest the following choices of materials. When designing for stiffness (E, G): i) as a f(T): low molecular weight (15880, 21180 g/mol) material up to 170°C. ii) as a f(Mw): high molecular weight (>25000 g/mol) material for all temperatures. When designing for strength (NTS): i) as a f(T): high molecular weight (51070, 41100 g/mol) material up to 140°C. ii) as a f(Mw): high molecular weight (>25000 g/mol) material for all temperatures.

Despite the uncertainty in quantifying the crosslink density and network properties in the PETI-SI materials, it has been shown that the effect of adding chain-terminated phenylethynyl reactive groups produces both thermally- and mechanically-stable materials at low molecular weights. More importantly, the results show that the inclusion of crosslinking causes a low molecular weight material to behave as a high molecular weight material.

5. ACKNOWLEDGEMENTS

The authors are grateful for the gel permeation chromatography performed by Dr. E. J. Siochi and the technical assistance of Mr. C. E. Townsley. This work was performed while LMN held a National Research Council Research Associateship at NASA Langley Research Center.

6. REFERENCES

1. A. K. Noor, *et al.*, in Aerospace America . (1998) pp. 24.
2. L. E. Nielsen, Mechanical properties of polymers and composites (Marcel Dekker, New York, 1974).
3. S. Matsuoka, Relaxation phenomena in polymers (Hanser, Munich, 1992).
4. D. J. Walsh and Y. Termonia, Polymer communications 29(April), 90 (1988).
5. D. Wilson, H. D. Stenzenberger and P. M. Hergenrother, Polyimides (Chapman and Hall, New York, 1990).
6. J. A. Johnston, *et al.*, Polymer 35(22), 4865 (1994).
7. B. J. Jensen and A. C. Chang, *High* Performance Polymers 10, 175 (1998).
8. B. J. Jensen, P. M. Hergenrother and G. Nwokogu, Polymer 34(3), 630 (1993).
9. J. A. Hinkley, Journal of Advanced Materials (April), 55 (1996).
10. P. M. Hergenrother, *et al.*, Journal of Polymer Science: Part A: Polymer Chemistry 32(16), 3061 (1994).
11. P. M. Hergenrother and J. G. Smith, Jr, Polymer 35(22), 4857 (1994).
12. X. Fang, *et al.*, Journal of Polymer Science: Part A: Polymer Chemistry 36, 461 (1998).
13. E. J. Siochi, P. R. Young and R. G. Bryant, Materials Challenge-Diversification and the Future 40(1) (SAMPE, Los Angeles, California, 1995).
14. R. G. Bryant, High Performance Polymers 8(4), 607 (1996).
15. T. H. Hou and R. G. Bryant, High Performance Polymers 9(4), 437 (1997).
16. T. Takekoshi and J. M. Terry, Polymer 35(22), 4874 (1994).
17. K. H. Wood, *et al.*, 42nd International SAMPE symposium (May, 1997).
18. A. Hale, C. W. Macosko and H. E. Bair, Macromolecules 24(9), 2610 (1991).
19. E. A. DiMarzio, Journal of research of the national bureau of standards - A. Physics and Chemistry 6(6), 611 (1964).
20. L. R. G. Treloar, The Physics of Rubber Elasticity, (Oxford University Press, London, ed. 3rd, 1975).
21. J. A. Hinkley and B. J. Jensen, High Performance Polymers 8, 599 (1996).
22. D. R. Miller and C. W. Macosko, Macromolecules 9(2), 206 (1976).
23. J. M. Pickard, E. G. Jones and I. J. Goldfarb, Macromolecules 12(5), 895 (1979).

A Short Biography of Lee M. Nicholson, Ph.D.

Lee studied in London, England for his B.Sc. degree in Applied Physics with Computing. Upon graduating with honors, he moved to the Cavendish Laboratory, University of Cambridge. He completed his Master of Philosophy degree, doing 'real' experimental physics. Lee gained an ICI Polymer Films fellowship to work on his Ph.D. with Prof. Alan Windle *FRS* in the department of Materials Science and Metallurgy, Cambridge. His doctoral thesis entitled, "Microstructural modeling of polymer films" simulated stress-induced crystallization in the biaxial drawing process. Since gaining a National Research Council fellowship, Lee is working on the mechanical properties of polymers at NASA Langley Research Center.